Journal of Biomedical Optics

BiomedicalOptics.SPIEDigitalLibrary.org

Quantitative Raman spectral changes of the differentiation of mesenchymal stem cells into islet-like cells by biochemical component analysis and multiple peak fitting

Xin Su
Shaoyin Fang
Daosen Zhang
Qinnan Zhang
Yingtian He
Xiaoxu Lu
Shengde Liu
Liyun Zhong

SPIE.

Quantitative Raman spectral changes of the differentiation of mesenchymal stem cells into islet-like cells by biochemical component analysis and multiple peak fitting

Xin Su, Shaoyin Fang, Daosen Zhang, Qinnan Zhang, Yingtian He, Xiaoxu Lu, Shengde Liu, and Liyun Zhong*
South China Normal University, Guangdong Provincial Key Laboratory of Nanophotonic Functional Materials and Devices, Science Building 4, Guangzhou 510006, Guangdong, China

Abstract. Mesenchymal stem cells (MSCs) differentiate into islet-like cells, providing a possible solution for type I diabetes treatment. To search for the precise molecular mechanism of the directional differentiation of MSC-derived islet-like cells, biomolecular composition, and structural conformation information during MSC differentiation, is required. Because islet-like cells lack specific surface markers, the commonly employed immunostaining technique is not suitable for their identification, physical separation, and enrichment. Combining Raman spectroscopic data, a fitting accuracy-improved biochemical component analysis, and multiple peaks fitting approach, we identified the quantitative biochemical and intensity change of Raman peaks that show the differentiation of MSCs into islet-like cells. Along with increases in protein and glycogen content, and decreases in deoxyribonucleic acid and ribonucleic acid content, in islet-like cells relative to MSCs, it was found that a characteristic peak of insulin (665 cm^{-1}) has twice the intensity in islet-like cells relative to MSCs, indicating differentiation of MSCs into islet-like cells was successful. Importantly, these Raman signatures provide useful information on the structural and pathological states during MSC differentiation and help to develop noninvasive and label-free Raman sorting methods for stem cells and their lineages. *© 2015 Society of Photo-Optical Instrumentation Engineers (SPIE)* [DOI: 10.1117/1.JBO.20.12.125002]

Keywords: medical optics; Raman spectroscopy; type 1 diabetes; islet-like cells; mesenchymal stem cells.

Paper 150313RR received May 12, 2015; accepted for publication Nov. 9, 2015; published online Dec. 16, 2015.

1 Introduction

Diabetes has become the third-most fatal disease and there is currently no cure.[1] In type I diabetes, caused by the absence of insulin production by pancreatic β cells (commonly known as islet-like cells), increasing the number of islet-like cells is an effective solution for treatment. Recently, research has shown that stem cell transplantation is a possible treatment for diabetes,[2–7] and several research groups have succeeded in the directional differentiation of embryonic stem cells (ESCs) or mesenchymal stem cells (MSCs) into islet-like cells.[5,8–10] Compared with ESCs, the procedures and applications of MSCs are ethically unchallenged. Moreover, it has been reported that MSC-derived islet-like cells reveal high similarity in structural and functional properties to pancreatic β cells *in vivo*.[8,11] Thus, MSCs act as an attractive *ex vivo* source of islet-like cells for cell-based type I diabetes treatment.[3,12–15] Though it has been found that some key transcription factors and signaling pathways might be required to induce the directional differentiation of MSCs into pancreatic β cells,[16–21] the precise molecular mechanism is not well described. Purifying the differentiated cells is an essential step for clinical application, as undifferentiated cells can lead to the formation of tumors after transplantation.[22] However, unlike conventional lineages, islet-like cells lack specific surface markers for the identification, physical separation, and enrichment by commonly employed immunostaining techniques (e.g., fluorescence-activated cell sorting or magnetic bead sorting).[23,24] Immunostaining by dithizone, which is a zinc-chelating agent known to selectively stain islet-like cells and requires permeabilization, renders differentiated cells unviable and nonrecoverable.

By measuring the vibration mode of intrinsic molecular bonds, Raman spectroscopy provides rich bimolecular composition and structural conformation information on individual living cells.[25,26] Due to several specific advantages, such as noninvasiveness, label-free use, and real-time data collection, Raman spectroscopy is a better candidate for the identification, physical separation, and enrichment of living cells. Purified biological macromolecules, such as deoxyribonucleic acid (DNA), ribonucleic acid (RNA), proteins, lipids, and polysaccharides, possess unique Raman peaks, but these macromolecules coexist in living cells and generate numerous peaks that overlap to form a broad band. As a result, it is not easy to determine the quantitative biochemical changes and the quantitative intensity changes of Raman peaks using only visual inspection.

Principal component analysis (PCA), a multivariate data analysis algorithm designed to reduce the variable number of a data set, provides abstract information representing entire features broadly distributed in a data set, but is limited to the explicit quantification of the biochemical changes of cells based on the Raman spectrum. Usually, cell-directional differentiation is performed by selectively activating and blocking different

*Address all correspondence to: Liyun Zhong, E-mail: zhongly@scnu.edu.cn

1083-3668/2015/$25.00 © 2015 SPIE

genes in a certain order, followed by the induction of protein synthesis by specific signaling pathways, and then generating the differentiated cell. Therefore, Raman spectral changes before and after differentiation provide useful information on the structural and pathological states of cells. Recently, biochemical component analysis (BCA) was introduced to estimate the spectral contribution of each biochemical component of cells,[27] in which the Raman spectrum is assumed to be the linear summation of all basic biochemical components. However, because BCA requires prior knowledge of the pure constituents of the sample to supply the fluorescence background model, it is sensitive to the variation of fluorescence background and limited in the inspection of peak shifts and variations in the relative intensity of peaks.

In this study, we developed a fitting accuracy-improved BCA approach to determine the quantitative biochemical changes before and after cell differentiation, in which three types of approximate fluorescence backgrounds, expressed either by the fifth-order polynomial fitting, the fourth-order polynomial fitting, or the penalized least-squares algorithm, were utilized as the corresponding three fitting factors to remove the fluorescence background from raw Raman spectra. Moreover, the multiple peaks fitting (MPF) approach was employed to calculate the quantitative intensity changes of Raman peaks for the differentiation of MSCs into islet-like cells.

2 Materials and Methods

2.1 *Differentiation of Mesenchymal Stem Cells into Islet-Like Cells*

Umbilical cords were provided by healthy newborns (approved by Guangdong provincial maternity and child care center), and MSCs were isolated as described previously.[25] After removing the cord vessels, umbilical cords were minced into 1-mm^3 fragments with sharp scissors under aseptic conditions. The fragments were washed with phosphate buffer saline (PBS) to remove contamination, and then treated with 0.2% collagenase II (Sigma) at 37°C for 2.5 h in a table concentrator. The digested mixture was first passed through a 100-μm filter and then a 200-μm filter to obtain cell suspensions. The dissociated cells were then washed with PBS, planted on uncoated T-25 culture flasks, and cultured in Dulbecco's modified Eagle's medium/Nutrient F12 Ham's 1:1 mixture (DMEM/F12 Gibco) and 10% fetal bovine serum (FBS, Gibco Australia). Finally, after 3 days of culture, the medium was replaced and nonadherent cells were removed. While the cells were at 90% confluence, they were passaged with 0.25% trypsin.

As shown in Fig. 1(a), many MSCs with a long spindle shape were observed in the proliferation medium, which was composed of DMEM/F12 supplemented with 10% FBS and 1% penicillin and streptomycin. Next, MSCs were cultured at a density of 3×10^5 cells/well in a 6-well plate for 5 days with pancreatic differentiation medium,[5] composed of DMEM/F12, 10 mM nicotinamide, 10 nM exendin-4, 10 nM pentagastrin, 100 pM hepatocyte growth factor, 2% B-27, and 2% N-2. As shown in Fig. 1(b), some floating cells with roughly spherical shapes were observed. While MSCs were cultured for 5 days, many floating cells with spherical shapes were observed [Fig. 1(c)]. Moreover, using a dithizone staining approach [Fig. 1(d)], these floating cells were shown to be islet-like cells, a type of pancreatic β cell.[5] MSCs were cultured in proliferation medium as the control group.

2.2 *Raman Spectroscopy and Data Preprocessing*

A Renishaw inVia Raman spectrometer attached to a Leica upright microscope equipped with a 50× objective, a 785 nm laser with a laser power of 50 mw, and a laser spot size of 2 μm, and a CCD detector with a spectral resolution of 0.99 cm^{-1} was utilized to collect Raman spectra of individual cells for all cell types, in which five different areas were randomly probed within a cell and the integration time for acquiring a Raman spectrum of a cell was 10 s in all experiments. A Raman spectrum of each cell type was expressed by an average of 10 cells in the scan range of 600 to 1800 cm^{-1}. Raman spectroscopic data processing was performed with MATLAB and Origin software, and the preprocessing procedure of the Raman spectrum was described in Fig. 2.

In this study, all spectra were normalized to the peak at 1655 cm^{-1}, which is predominantly related to protein and lipid, to perform a direct comparison of the data. In the reported

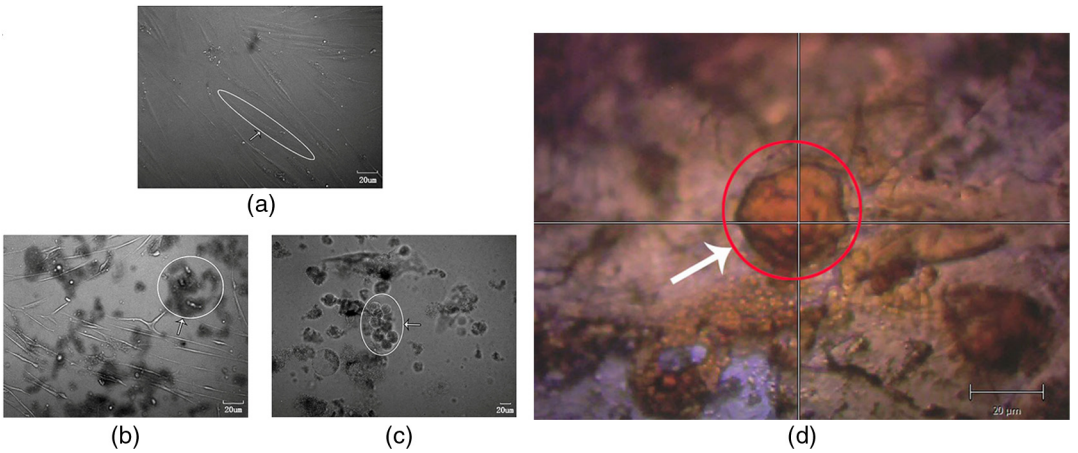

Fig.1 Bright-field images of mesenchymal stem cells (MSCs) differentiating into islet-like cells. (a) Many MSCs (white circle) with long spindle shapes were observed before differentiation. (b) Some floating cells appeared on the fourth day of differentiation (white circle). (c) Some islet-like cells appeared on the fifth day of differentiation (white circle). (d) Fluorescence image of islet-like cells stained by dithizone (red circle).

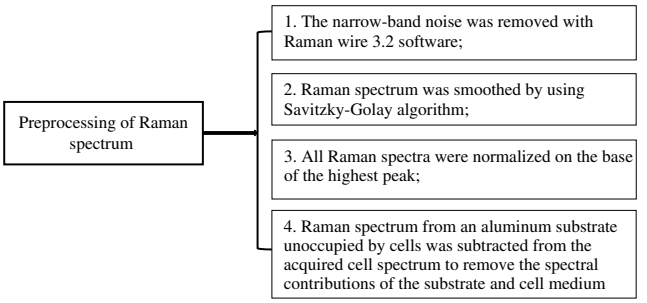

Fig. 2 The preprocessing procedure of Raman spectrum.

BCA fitting,[27] seven basic components—actin, albumin, triolein, phosphatidylcholine, DNA, RNA, and glycogen—were employed as the major organic molecules of biological cells, in which actin and albumin were attributed to proteins; triolein and phosphatidylcholine were attributed to lipids; glycogen was attributed to polysaccharides; and DNA and RNA were attributed to nucleic acids. The procedure of the reported BCA fitting was described in Fig. 3.

As shown in Fig. 4, from the raw Raman spectrum of MSCs or islet-like cells, it was found that the signal-to-noise ratio (SNR) for several main peaks at 1004, 1448, 1655 cm^{-1} was more than 50:1, and even in these low-intensity peaks, such as 665 cm^{-1}, the SNR was more than 10:1, indicating our Raman spectroscopic data are suitable for the quantitative analysis. In this study, we also chose the above seven biochemical components to perform the BCA operation, and the corresponding fitting results of MSCs and islet-like cells as in Fig. 4(a). It was shown that the correlation coefficient between the fitting spectrum and the raw spectrum was less than 90%, showing that the BCA fitting accuracy with the reported direct background subtraction approach is relatively low. One main reason is that the fluorescence background of biological samples is varied and unstable. To solve this problem, we employed three types of approximate fluorescence backgrounds, which were expressed either by the fifth-order polynomial fitting, the fourth-order polynomial fitting, or the penalized least-squares fitting.[28] As shown in Fig. 4(b), the correlation coefficient between the fitting Raman spectrum and the raw Raman spectrum was more than 97%, indicating a greatly improved fitting accuracy with the proposed BCA operation. The ratio of the fitting coefficient of each biochemical component to the sum of all fitting coefficients (excluding the coefficients from the three fluorescence backgrounds) was also obtained. Then the relative contribution of each basic biochemical component to the cell spectrum was determined (Fig. 4). Similarly, the final fitting fluorescence background could be obtained by the summation

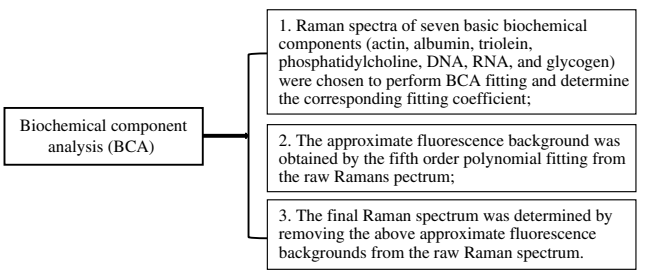

Fig. 3 The procedure of the reported biochemical component analysis (BCA) fitting.

of each fluorescence background multiplied by its fitting coefficient. Taking the MSCs spectrum as an example, the fitting fluorescence background is shown in Fig. 5 (green line). After removing the fluorescence background, we obtained the final fitting Raman spectrum of MSCs (Fig. 5, red line). For the sake of comparison, the final fitting Raman spectra of MSCs and islet-like cells are presented in Fig. 6.

3 Results and Discussion

3.1 *Raman Data Analysis with Biochemical Component Analysis and Multiple Peaks Fitting*

Using the improved BCA approach, we first obtained the quantitative biochemical changes before and after MSC differentiation [Fig. 4(c)], in which the error bar represented the standard deviation (SD) of the fitting coefficients measured in 10 cells. A Wilcoxon signed-rank test showed differences in all components between these two differentiated modes ($P < 0.05$). In addition, to verify the reliability of the above BCA results, we also measured the relative content changes of biochemical constituents between MSCs and islet-like cells by using five-kind conventional biochemical methods, as shown in Table 1. As is known, it was very difficult to obtain the percentages of each biochemical constituent or the relative content changes of all biochemical constituents by a one-kind biochemical examination method. Therefore, the measured value, representing the content of each biochemical constituent, was given as the relative value of control. Data were expressed as mean $\pm$ SD from three independent experiments, with significant differences from control designated as $^{*}P < 0.05$ and $^{**}P < 0.01$. Cellular actin content was obtained by the Western blot analysis. Total protein was extracted and electrophoresed using sodium dodecyl sulfate polyacrylamide gel electropheresis (SDS-PAGE) and polyvinylidene fluoride (PVDF) membranes (Merck-Millipore). The chemiluminescence signal was imaged using ChemiDoc XRS (Bio-Rad) and quantified using Image J. Cellular albumin content was measured by the bromocresol green assay kit (Sigma–Aldrich, Germany) according to the manufacturer's instructions. Cellular phosphatidylcholine and glycogen contents were, respectively, assessed using the commercially available kits (BioVision) according to manufacturer's instructions. The total RNA of MSCs or islet-like cells was extracted for cDNA synthesis; the generated cDNAs were analyzed by a quantitative real-time polymerase chain reaction (TRIzol reagent, Invitrogen). RNA purity and concentration were determined using a spectrophotometer (Ultrospec 2100 pro UV/Visible, Amersham Bioscience, Germany). Cellular triolein content was detected by the above spectrophotometer, in which the purified triolein was obtained from Perimed Crop. (Beijing, China). Cellular DNA content was measured by DNA-image cytometry, in which MSCs or islet-like cells and the controls were stained using the Feulgen reaction and assessed for integrated optical density by image analysis, and the ploidy status was assessed.

From Fig. 4 and Table 1, we can see that the relative content changes of biochemical constituents between MSCs and islet-like cells with the proposed BCA method were closely consistent with the conventional biochemical methods, indicating that the employed seven basic biochemical components were suitable for the BCA operation of MSCs' differentiation.

Moreover, we also introduced an MPF approach to quantify the intensity changes of Raman peaks, in which the profile of

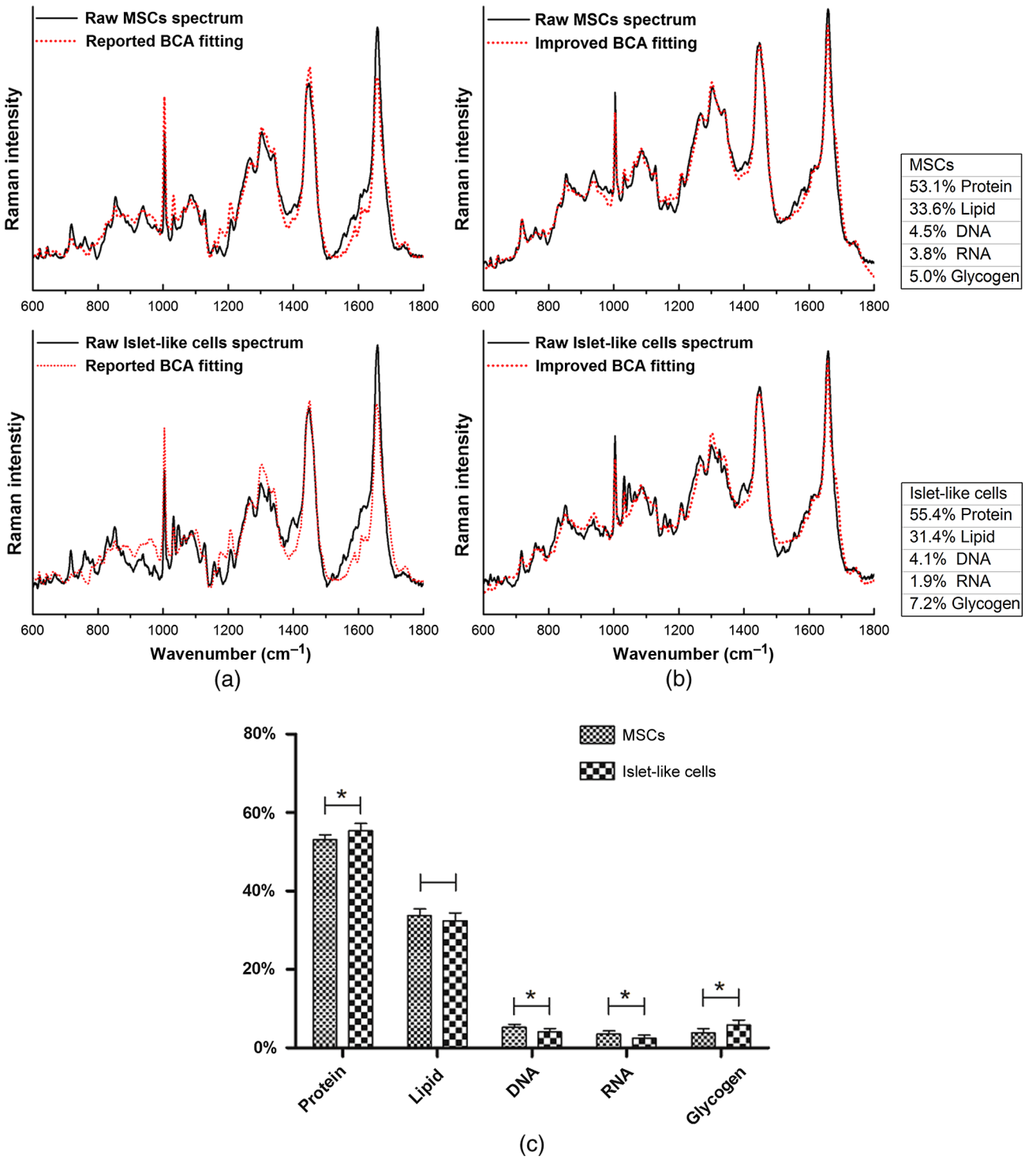

Fig.4 BCA fitting results with two different approaches. (a) The poorness of the BCA fitting result in which the background was directly subtracted from the raw Raman spectrum. (b) The goodness of the BCA fitting result in which three approximate fluorescence backgrounds were used as BCA fitting factors. (c) Spectrum contribution of each biochemical component with the improved BCA approach. Asterisk indicates a significance level of $P < 0.05$.

each Raman peak was considered a Gaussian curve.[25] As shown in Fig. 7, the correlation coefficient between MPF and the raw Raman spectrum was greater than 99%. As a result, we can easily determine the accurate intensity changes of each Raman peak. This good MPF result shows that the fluorescence background embedded in the raw Raman spectrum has been effectively eliminated by using the accuracy-improved BCA approach. Like the differentiation of other cells,[10,22,29] Raman spectral changes during the differentiation of MSCs into islet-like cells also reflect their active cell cycles and the extent of protein synthesis. For example, the decreased RNA content in islet-like cells relative to MSCs suggests a lower translational

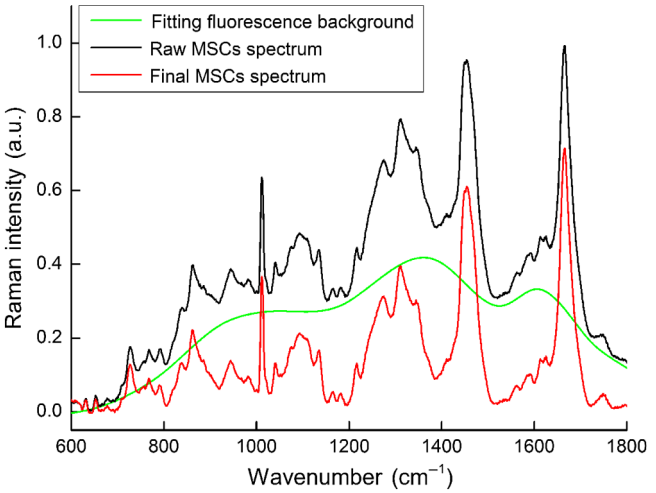

Fig. 5 Fitting fluorescence background obtained by the improved BCA operation (green line) and the final Raman spectrum of MSCs (red line).

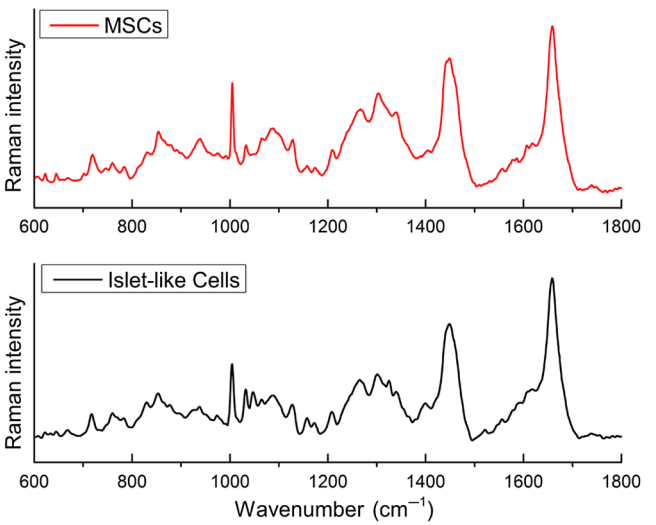

Fig. 6 Final Raman spectra of MSCs (red line) and islet-like cells (black line) obtained by the improved BCA approach.

rate of mRNA in these undifferentiated cells; accordingly, the protein content in islet-like cells was slightly higher than that in MSCs. The lower DNA content in islet-like cells may be indicative of the lower proliferation of these differentiated cells due to their development into a more mature phenotype. Moreover, the increase of glycogen content in islet-like cells relative to MSCs shows that differentiation is an active process that requires energy. Specially, note that two peaks at 1047 cm^{-1} (unassigned) and 1322 cm^{-1} (assigned to protein) were not observed in the BCA fitting result [Fig. 4(b)], suggesting that a new biochemical component not attributed to the seven basic biochemical components might exist in MSCs and their differentiated cells.

Next, combining the accuracy-improved BCA fitting and MPF results, we performed a quantitative comparison of the biochemical component and intensity changes of Raman peaks before and after MSC differentiation. Interestingly, as shown in Fig. 7 and Table 2, we can see that five peaks at 623, 644, 665, 784, and 1090 cm^{-1} were assigned to DNA, but four peaks at 623, 644, 784, and 1090 cm^{-1} were lower in intensity in islet-like cells than in MSCs. One peak at 665 cm^{-1} in islet-like cells had nearly twice the intensity as that in MSCs. It is impossible to determine the quantitative changes in DNA content by the intensity changes of Raman peaks using the MPF approach. However, using BCA fitting (Fig. 4), we can determine the decrease in DNA content after differentiation. It has been reported that a lower DNA content might be indicative of a lower proliferation of differentiated cells,[22,29] suggesting that our islet-like cells have developed into a more mature phenotype.

Subsequently, we also observed that the peak at 811 cm^{-1} assigned to RNA was higher in intensity in MSCs than in islet-like cells (Fig. 7). This is because once the functional mature cell is generated after differentiation, its RNA content will be lowered following mRNA transcription and protein synthesis.[22] MSCs are human progenitor cells and, before they become functional mature cells, their synthetic protein content is less than that in islet-like cells. Thus, the lower transcription rate of mRNA in MSCs leads to a higher RNA content in MSCs relative to islet-like cells. Moreover, various synthetic proteins are required to induce the generation of islet-like cells. Therefore, the RNA content in islet-like cells is lower than that in MSCs. Our BCA fitting result also demonstrates that the RNA content decreased after differentiation.[22,29,30] Furthermore,

Table 1 Relative content changes of biochemical constituents between mesenchymal stem cells (MSCs) and islet-like cells.

Biochemical constituents	Protein		Lipid		Deoxyribonucleic acid (DNA)	Ribonucleic acid (RNA)	Glycogen
	Actin	Albumin	Phosphatidylcholine	Triolein			
Methods or reagents	Western blot	Bromocresol green	Assay kit	Spectrophotometry	Image cytometry	Quantitative real-time polymerase chain reaction	Assay kit
MSCs	$6.21 \pm 0.51^{*}$	$72.97 \pm 5.75^{*}$	$46.22 \pm 5.45^{*}$	$39.21 \pm 4.37^{*}$	$1.54 \pm 0.49^{*}$	$1.48 \pm 0.28^{**}$	$13.66 \pm 2.92^{*}$
Islet-like cells	$6.24 \pm 0.83^{*}$	$75.18 \pm 4.61^{*}$	$44.79 \pm 3.82^{*}$	$38.72 \pm 2.95^{*}$	$1.53 \pm 0.65^{*}$	$1.42 \pm 0.57^{**}$	$14.82 \pm 1.47^{*}$
Relative content changes (%)	$0.39 \pm 0.47^{*}$	$2.94 \pm 1.38^{*}$	$-3.19 \pm 1.36^{*}$	$-1.27 \pm 0.81^{*}$	$-0.65 \pm 0.22^{*}$	$-4.23 \pm 0.45^{**}$	$7.82 \pm 2.16^{*}$
	$3.33 \pm 0.92^{*}$		$-4.46 \pm 1.15^{*}$				

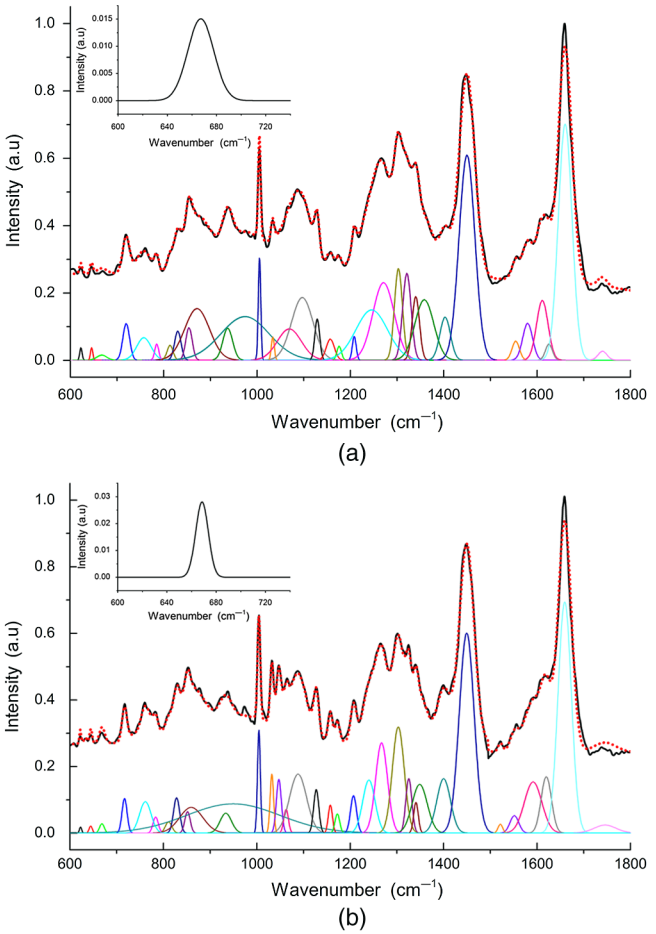

Fig. 7 Multiple peaks fitting (MPF) results of (a) MSCs; (b) islet-like cells, in which the black line and red dashed line (the upper row) represent the actual Raman spectra and the spectra obtained with the MPF fitting approach, respectively, and the other colored lines (the lower row) represent the different Gaussian fitting peaks. The upper left insets represent the zoomed image of the black square area of MSCs or islet-like cells spectra around the peak at 665 cm^{-1}.

with the exception of the collagen peaks at 1322 and 1347 cm^{-1}, the other peaks at 758, 830, 1030, 1157, 1174, and 1208 cm^{-1} (assigned to proteins) were more prominent in the differentiated cells. Our BCA operation also showed that the protein content was slightly increased after differentiation. Similar to other reports of cell differentiation,[22,29] our BCA fitting showed that an increase in protein content and a decrease in DNA content were observed during the differentiation of MSCs into islet-like cells, so the peak intensity ratio of protein to nucleic acid (such as 758 cm^{-1}/784 cm^{-1}) was increased after differentiation.

Note that the intensity increase of the three peaks at 1004, 1030, and 1208 cm^{-1} assigned to phenylalanine (Phe) was also observed after differentiation, in which Phe is an important cell factor for inducing insulin generation.[31–33] In particular, an intensity increase of the peak at 1267 cm^{-1}, which was assigned to amide III and related to changes in protein secondary structure,[34] was observed after differentiation, indicating that the type of synthetic protein in the amide III region might be changed after differentiation. Importantly, the peak at 665 cm^{-1} assigned to DNA, as described in Refs. 35 and 36, should be decreased or unchanged in intensity after differentiation. However, as shown in Fig. 7, our MPF result revealed that the intensity of the peak at

Table 2 Raman peak frequencies and their assignments.

	Raman frequency (cm^{-1})	Assignment
1	623	A five-member ring deformation
2	644	T ring angle bend
3	665	T,G ring breath
4	758	Trp ring breath
5	784	U,C,T ring breath., O—P—O str
6	811	O—P—O str of RNA
7	830	Tyr out of plane ring breath (p)
8	870	C—C symm str in lipid
9	1004	Phe symm ring breath
10	1030	Phe C—H in-plane (p)
11	1064	Chain C—C str in lipids
12	1090	C—C stretch, O—P—O stretch (nucleic acids)
13	1157	C—C/C—N str (p)
14	1174	Tyr,Phe (p)
15	1208	C – C_6H_5 str of Phe
16	1267	Amide III
17	1322	G, CH def in proteins
18	1347	CH def in protein
19	1448	CH def in DNA/RNA, proteins, lipids, and carbohydrates
20	1655	Amide I-band vibrations (p)

Note: Abbreviations: p, protein; A,G,T,C,U, ring breathing modes of DNA/RNA; str, stretching; breath., breathing; Phe, phenylalanine; and Tyr, tyrosine.

665 cm^{-1} was about twice as much in islet-like cells as that in MSCs, while a decrease in the total DNA content was observed after differentiation. A possible explanation is that the peak at 665 cm^{-1}, which has been demonstrated as a characteristic peak of insulin,[37–39] is produced by islet-like cells. Because the amount of insulin produced by MSC-derived islet-like cells is relatively low,[8,11,40] the peak at 665 cm^{-1} was lower in intensity than those Raman peaks between 1000 and 1100 cm^{-1} or around 1300 cm^{-1}. Subsequently, we also observed that other DNA peaks at 623, 644, 784, and 1090 cm^{-1} were lower in intensity after differentiation. Collectively, along with the decrease in DNA content, we conclude that the increased intensity of the peak at 665 cm^{-1} after differentiation is induced by insulin generation, further indicating that the directional differentiation of MSCs into islet-like cells was successful. It should be reasonable to utilize the intensity increase of the peak at 665 cm^{-1} as a marker for the identification, physical separation, and enrichment of islet-like cells. Of course, several other peaks at 830, 1030, and 1174 cm^{-1}, which are observed in the

spectrum of insulin,[37] were also more prominent in islet-like cells than in MSCs. Similarly, we also can also use these peaks as characteristic parameters for the generation of islet-like cells.

It is well known that glucose serves as a rapid energy source. Our BCA fitting showed that glycogen content was increased after differentiation, indicating that glucose served as the energy source for the differentiation of MSCs into Islet-like cells. By combining the improved BCA and MPF approaches, we determined the quantitative biochemical changes and the quantitative intensity changes of Raman peaks for MSC differentiation into islet-like cells.

3.2 *Raman Data Analysis with Principal Component Analysis*

To assess the discrimination of MSCs and their differentiated cells, we employed PCA to compare the background-subtracted and normalized Raman spectra of different groups in this study. In PCA, if one type of cells is separated into the same cluster, then the scatter plot generated from this group data represents the same type of cells.[41] Because the first few principal components (PCs) and the corresponding loading values for each PC contain most of the spectral information of the raw Raman data, each spectrum can be expressed as a linear combination of the first few PCs. As shown in Fig. 8, we first constructed two-dimensional plots with different combinations of scores for the first three PCs [Figs. 8(a)–8(c)] and three-dimensional plots with three sets of scores [Fig. 8(d)]. Interestingly, it was observed that the first three PCs accounted for approximately 85% of the total spectral information. Because protein is the main component of biological cells and PC1 accounted for 55% of the total spectral information, the spectral profile of PC1 is very similar to the actual cell spectrum [Figs. 8(a) and 9]. Moreover, it was seen that cells before and after differentiation were separated into two distinct clusters in PC1, indicating that

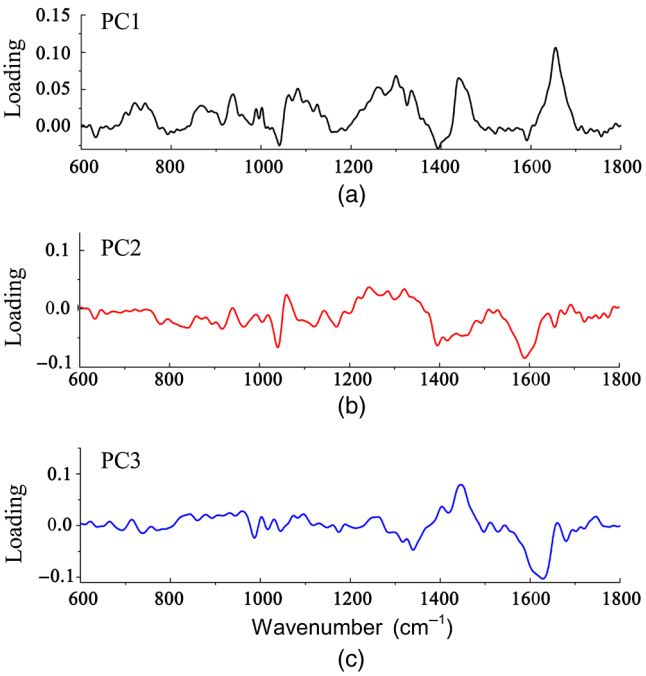

Fig. 9 Spectra of the first three principal components in PCA: (a) PC1, (b) PC2, and (c) PC3.

the discrimination of proteins before and after differentiation can be determined by PC1. However, using BCA fitting (Fig. 4), no obvious changes in protein content were observed, indicating that PC1 is not just composed of protein. As shown in Fig. 7 and Table 2, some of these peaks assigned to proteins increased in intensity while others decreased in intensity, and one possible explanation is that conformational changes in some proteins occurred.

As described in the above analysis, we can see that the data classification with BCA is different from that with PCA. The

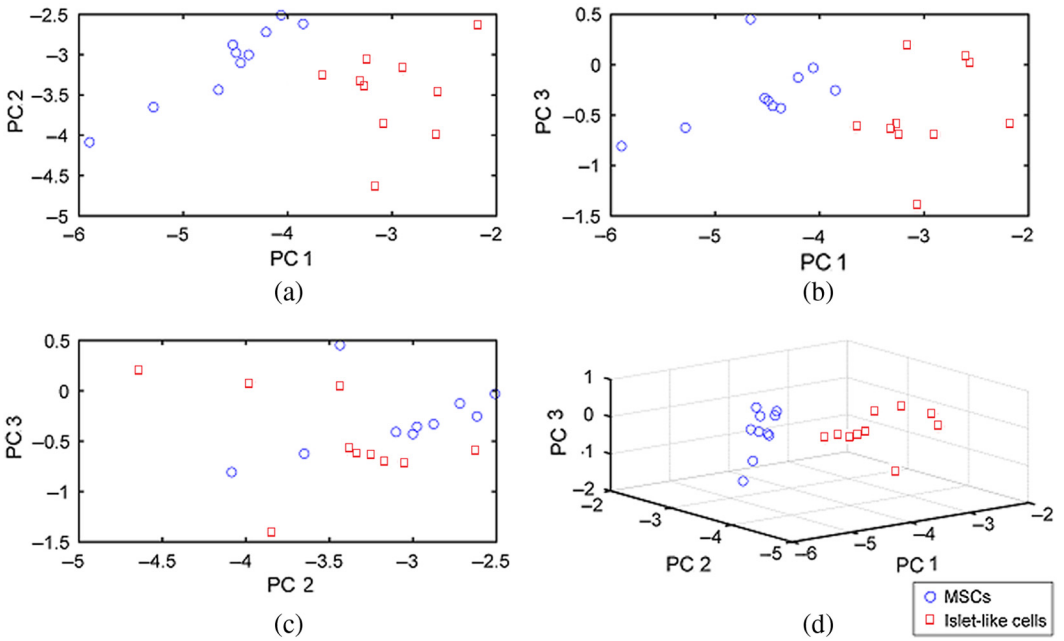

Fig. 8 (a)–(c) Two-dimensional principal component analysis (PCA) scatter plots of the first two PCs, (d) three-dimensional PCA scatter plot, in which the contributions of PC1, PC2, and PC3 were 55%, 19%, and 11%, respectively.

former is performed by the content changes of biochemical components, while the latter is performed by the spectral changes of Raman peaks. Even if the biochemical component content is not changed, when the structure of the biochemical component is changed, its corresponding Raman peaks will be changed. Thus, BCA is suitable for revealing the biochemical changes of cells, while PCA can supply the discrimination information of different type cells.

PC2 and PC3 accounted for only 19% and 11%, respectively, of the total spectral information [Figs. 8(a) and 8(b)], so it was difficult to assess the discrimination between MSCs and the differentiated cells with PC2 or PC3. As a result, we can see that there was a large discrimination between PC2 or PC3 and the actual cell spectrum (Fig. 9). Although the PC2 spectrum captured a peak 1064 cm^{-1}, changes in the lipid content before and after differentiation were observed by BCA fitting. However, PC2 accounted for 19% of the total spectral information, so the discrimination of different cell groups in PC2 was less than that in PC1. Similarly, the discrimination of different cell types in PC3 was much less.

4 Conclusion

Increased numbers of islet-like cells may become an effective treatment solution for type I diabetes. Though it has been reported that MSCs can be differentiated into islet-like cells[5,10] and have the potential to act as an attractive *ex vivo* source of these cells, islet-like cells lack specific surface markers, and the commonly employed immunostaining technique is not suitable for their identification, physical separation, and enrichment. Though it has been reported that some key transcription factors and signaling pathways might be required to induce the directional differentiation of MSCs into pancreatic β cells,[16–21] the precise molecular mechanism is not well described. Thus, the accurate regulation of MSC-derived islet-like cell generation and its clinical application is greatly limited. In this study, combining Raman spectroscopic data, a fitting accuracy-improved BCA operation, and an MPF approach, the quantitative biochemical and intensity changes of Raman peaks for MSC differentiation into islet-like cells were determined. Interestingly, the peak at 665 cm^{-1}, which has been demonstrated as one of the characteristic peaks of insulin produced by islet-like cells,[37] was increased twofold in islet-like cells relative to MSCs. The above results provide evidence demonstrating that the directional differentiation of MSCs into islet-like cells has been successful, and the intensity increase of the peak at 665 cm^{-1} can be utilized as a marker for the identification, physical separation, and enrichment of MSC-derived islet-like cells. Importantly, Raman signatures provide useful information on the structural and pathological states of cells and help to develop a noninvasive and label-free Raman sorting method for stem cells and their lineages. In addition, the discrimination of different types of cells using PCA is convenient.

Acknowledgments

This work was supported by the National Nature Science Foundation of China (Grants 61078064 and 61275015).

References

1. M. Williams et al., "Hemodialyzed type I and type II diabetic patients in the US: characteristics, glycemic control, and survival," *Kidney Int.* **70**, 1503–1509 (2006).
2. K. Docherty, A. S. Bernardo, and L. Vallier, "Embryonic stem cell therapy for diabetes mellitus," *Semin. Cell Dev. Biol.* **18**, 827–838 (2007).
3. K. C. Chao et al., "Islet-like clusters derived from mesenchymal stem cells in Wharton's Jelly of the human umbilical cord for transplantation to control type 1 diabetes," *PLoS One* **3**, e1451 (2008).
4. L. Vija et al., "Mesenchymal stem cells: stem cell therapy perspectives for type 1 diabetes," *Diabetes Metab.* **35**, 85–93 (2009).
5. S. Dave, A. Vanikar, and H. Trivedi, "Extrinsic factors promoting in vitro differentiation of insulin-secreting cells from human adipose tissue-derived mesenchymal stem cells," *Appl. Biochem. Biotechnol.* **170**, 962–971 (2013).
6. L. Yang et al., "In vitro trans-differentiation of adult hepatic stem cells into pancreatic endocrine hormone-producing cells," *Proc. Natl. Acad. Sci. U. S. A.* **99**, 8078–8083 (2002).
7. K. D. McKnight, P. Wang, and S. K. Kim, "Deconstructing pancreas development to reconstruct human islets from pluripotent stem cells," *Cell Stem Cell* **6**, 300–308 (2010).
8. N. Lumelsky et al., "Differentiation of embryonic stem cells to insulin-secreting structures similar to pancreatic islets," *Science* **292**, 1389–1394 (2001).
9. J. K. Mfopou et al., "Recent advances and prospects in the differentiation of pancreatic cells from human embryonic stem cells," *Diabetes* **59**, 2094–2101 (2010).
10. L. F. Wu et al., "Differentiation of Wharton's jelly primitive stromal cells into insulin-producing cells in comparison with bone marrow mesenchymal stem cells," *Tissue Eng. Part A* **15**, 2865–2873 (2009).
11. F. Gao et al., "In vitro cultivation of islet-like cell clusters from human umbilical cord blood-derived mesenchymal stem cells," *Transpl. Res.* **151**, 293–302 (2008).
12. R. Abdi et al., "Immunomodulation by mesenchymal stem cells a potential therapeutic strategy for type 1 diabetes," *Diabetes* **57**, 1759–1767 (2008).
13. C. G. Fan, Q. J. Zhang, and J. R. Zhou, "Therapeutic potentials of mesenchymal stem cells derived from human umbilical cord," *Stem Cell Rev. Rep.* **7**, 195–207 (2011).
14. R. R. Taghizadeh, K. J. Cetrulo, and C. L. Cetrulo, "Wharton's jelly stem cells: future clinical applications," *Placenta* **32**, S311–S315 (2011).
15. R. Anzalone et al., "Wharton's jelly mesenchymal stem cells as candidates for beta cells regeneration: extending the differentiative and immunomodulatory benefits of adult mesenchymal stem cells for the treatment of type 1 diabetes," *Stem Cell Rev. Rep.* **7**, 342–363 (2011).
16. H. J. Yuan et al., "Expression of Pdx1 mediates differentiation from mesenchymal stem cells into insulin-producing cells," *Mol. Biol. Rep.* **37**, 4023–4031 (2010).
17. G. K. C. Brolén et al., "Signals from the embryonic mouse pancreas induce differentiation of human embryonic stem cells into insulin-producing β-cell-like cells," *Diabetes* **54**, 2867–2874 (2005).
18. J. M. Oliver-Krasinski et al., "The diabetes gene Pdx1 regulates the transcriptional network of pancreatic endocrine progenitor cells in mice," *J. Clin. Invest.* **119**, 1888–1898 (2009).
19. C. Cras-Méneur et al., "Presenilins, Notch dose control the fate of pancreatic endocrine progenitors during a narrow developmental window," *Genes Dev.* **23**, 2088–2101 (2009).
20. M. F. Rath et al., "Developmental and daily expression of the Pax4 and Pax6 homeobox genes in the rat retina: localization of Pax4 in photoreceptor cells," *J. Neurochem.* **108**, 285–294 (2009).
21. Y. H. You et al., "Adenoviruses expressing PDX-1, BETA2/NeuroD and MafA induces the transdifferentiation of porcine neonatal pancreas cell clusters and adult pig pancreatic cells into β-cells," *Diabetes Metab. J.* **35**, 119–129 (2011).
22. J. W. Chan et al., "Label-free separation of human embryonic stem cells and their cardiac derivatives using Raman spectroscopy," *Anal. Chem.* **81**, 1324–1331 (2009).
23. M. F. Pera et al., "Regulation of human embryonic stem cell differentiation by BMP-2 and its antagonist noggin," *J. Cell Sci.* **117**, 1269–1280 (2004).
24. X. P. Zhou et al., "Isolation, cultivation and identification of brain glioma stem cells by magnetic bead sorting," *Neural Regen. Res.* **7**, 985–992 (2012).
25. H. Bai et al., "Detecting viability transitions of umbilical cord mesenchymal stem cells by Raman micro-spectroscopy," *Laser Phys. Lett.* **8**, 78–84 (2011).

26. G. B. Jung et al., "A simple and rapid detection of tissue adhesive-induced biochemical changes in cells and DNA using Raman spectroscopy," *Biomed. Opt. Express* **4**, 2673–2682 (2013).
27. Y. H. Ong, M. Lim, and Q. Liu, "Comparison of principal component analysis and biochemical component analysis in Raman spectroscopy for the discrimination of apoptosis and necrosis in K562 leukemia cells," *Opt. Express* **20**, 22158–22171 (2012).
28. Z. M. Zhang et al., "An intelligent background-correction algorithm for highly fluorescent samples in Raman spectroscopy," *J. Raman Spectrosc.* **41**, 659–669 (2010).
29. H. G. Schulze et al., "Assessing differentiation status of human embryonic stem cells noninvasively using Raman microspectroscopy," *Anal. Chem.* **82**, 5020–5027 (2010).
30. C. Aksoy and F. Severcan, "Role of vibrational spectroscopy in stem cell research," *Spectrosc. Int. J.* **27**, 167–184 (2012).
31. J. F. Iverson, M. C. Gannon, and F. Q. Nuttall, "Ingestion of leucine + phenylalanine with glucose produces an additive effect on serum insulin but less than additive effect on plasma glucose" *J. Amino Acids* **2013**, 964637 (2013).
32. J. C. Floyd, Jr. et al., "Stimulation of insulin secretion by amino acids," *J. Clin. Invest.* **45**, 1487 (1966).
33. L. J. van Loon et al., "Amino acid ingestion strongly enhances insulin secretion in patients with long-term type 2 diabetes," *Diabetes Care* **26**, 625–630 (2003).
34. H. Kinoshita et al., "Phosphate and amide III mapping in sialoliths with Raman microspectroscopy," *J. Raman Spectrosc.* **39**, 349–353 (2008).
35. L. L. McManus et al., "Raman spectroscopic monitoring of the osteogenic differentiation of human mesenchymal stem cells," *Analyst* **136**, 2471–2481 (2011).
36. F. C. Pascut et al., "Non-invasive label-free monitoring the cardiac differentiation of human embryonic stem cells in-vitro by Raman spectroscopy," *Biochim. Biophys. Acta* **1830**, 3517–3524 (2013).
37. J. Hilderink et al., "Label-free detection of insulin and glucagon within human islets of Langerhans using Raman spectroscopy," *PLoS One* **8**, e78148 (2013).
38. X. Rong, S. S. Huang, and X. C. Kuang, "Real-time detection of single-living pancreatic beta-cell by laser tweezers Raman spectroscopy: high glucose stimulation," *Biopolymers* **93**, 587–594 (2010).
39. M. M. Gabr et al., "Generation of insulin-producing cells from human bone marrow-derived mesenchymal stem cells: comparison of three differentiation protocols," *Biomed Res. Int.* **2014**, 832736 (2014).
40. O. Karnieli et al., "Generation of insulin-producing cells from human bone marrow mesenchymal stem cells by genetic manipulation," *Stem Cells* **25**, 2837–2844 (2007).
41. M. Lasalvia, G. Perna, and V. Capozzi, "Raman spectroscopy of human neuronal and epidermal cells exposed to an insecticide mixture of chlorpyrifos and deltamethrin," *Appl. Spectrosc.* **68**, 1123–1131 (2014).

Liyun Zhong's current research is focused on investigating T cell activation and signal transduction using new imaging techniques with high resolution; and developing and applying new optical imaging techniques to study the behavior of individual biological molecules and live cells.

Biographies for the other authors are not available.